12th IEA Heat Pump Conference 2017

Parameter Estimation and Uncertainty Assessment of Thermal Response Test Using Bayesian Approach

Wonjun Choi[a]*, Hideki Kikumoto[a], Ruchi Choudhary[b], Ryozo Ooka[a]

[a]Institute of Industrial Science, The University of Tokyo, 4-6-1, Komaba, Meguro-ku, Tokyo 153-8505, Japan
[b]Efficient Cities Initiative, Department of Engineering, University of Cambridge, Trumpington Street, Cambridge CB2 1PZ, UK

Abstract

In order to design a borehole heat exchanger (BHE), which forms the main component of a ground source heat pump (GSHP), two parameters should be known: the effective thermal conductivity of the ground and the borehole thermal resistance. These parameters are estimated by conducting in situ thermal response tests (TRTs). TRTs are conducted in outdoor environments and thus affected by many disturbance factors. Although the estimation may contain significant uncertainty, these two parameters are mostly estimated via a deterministic approach. Considering the impact of the parameters on the initial cost of the GSHP, the estimates as well as their uncertainty should be concurrently evaluated. Thus, in this study, we develop a probabilistic estimation method based on Bayes' theorem that can provide the parameter estimates and their confidence intervals. Via comparison of our approach with a deterministic method, we identify the advantages of the Bayesian inference method.

© 2017 Stichting HPC 2017.
Selection and/or peer-review under responsibility of the organizers of the 12th IEA Heat Pump Conference 2017.

Keywords: Thermal response test; Ground source heat pump; Parameter estimation; Bayesian inference; Uncertainty assessment

* Corresponding author. Tel.: +81-3-5452-6435; fax: +81-3-5452-6432.
E-mail address: wonjun@iis.u-tokyo.ac.jp

1. Introduction

In comparison with air, the ground has a considerably larger thermal capacity and thus maintains a stable temperature. In this context, the ground source heat pump (GSHP) that utilizes the ground's characteristic as a heat source/sink has found wide spread use. To determine the appropriate size of the borehole heat exchanger (BHE) that is a main component of GSHP, the effective thermal conductivity of the ground and the borehole thermal resistance are required to be known. Because the ground is a composite medium, it is difficult to obtain reliable thermal conductivity values. Therefore, the abovementioned parameters are inversely estimated by means of conducting an in situ thermal response test (TRT). However, even when the parameters are estimated via a TRT, the results can contain significant uncertainty because of the intrinsic error of the sensors and disturbances from the ambient environment. Nevertheless, TRT data are mostly interpreted with the use of deterministic methods without providing the uncertainty of estimated parameters.

In this backdrop, in this study, we propose a probabilistic estimation method based on Bayes' theorem that can provide the relevant parameter estimates and their uncertainties concurrently. Because we cannot know the true value from in situ TRT, we numerically generate TRT data using a finite element method (FEM). We apply the intrinsic random error of the sensors to the numerical TRT data and consider them as measured data. Using the measured data, we estimate the parameters of interest (i.e., the effective thermal conductivity, borehole thermal resistance, and error ratio of measurement) with the Bayesian inference method and obtain their probability density functions. Because of the ill-posedness of the inverse parameter estimation, we apply a two-step Bayesian inference technique. Based on the results, we identify the advantages of our method over a conventional deterministic estimation method.

2. Generation of Measured TRT Data

TRT data were numerically generated with the use of an FEM. The calculation domain had dimensions of 15 × 15 × 80 m (length × width × depth). The geometry of the BHE and thermal properties of each component are listed in Table 1. The numerical model only considered the heat conduction, and the thermal properties were homogeneous and constant. The geometry of the BHE was fully discretized and the fluid flow inside the U-tube was modeled based on a 1D flow element. The detailed modeling method of the 1D flow element can be found in Ref. [1]. The heat injection rate and flow rate were set to 2.5 kW (50 W/m) and 15 L/min, respectively. The initial ground temperature of 17 °C was assigned to the whole calculation domain. The adiabatic boundary condition was assigned to the top and lateral surfaces and the Dirichlet boundary condition of 17 °C was assigned to the bottom surface. The inlet boundary of the U-tube was set as a time-varying Dirichlet condition based on the outlet temperature of previous time step, heat injection rate, and flow rate. The simulation was conducted for an elapsed time of 96 h with a time step of 6 min. For the parameter estimation, the data at 1-h intervals were used.

The general random error of the sensor was applied to the numerically generated TRT data. We used a Pt100 sensor for the inlet and outlet temperatures, whose accuracy was $\pm 0.15 + 0.002 \cdot T$ [°C], corresponding to the general accuracy of Class A sensors. For the flow meter, we assumed an electromagnetic flow meter that has a random error of ±0.5%. In contrast to the temperature sensor that reads an instantaneous value, the flow rate of the TRT is relatively constant, and thus, an averaged value from multiple independent sensing values can be used. Assuming that the measurement at 20-s intervals and TRT data at 1-h intervals were used for the parameter estimation, we obtained an accuracy of $\pm 0.6/\sqrt{180}\%$ based on the central limit theorem. Using these measured data sets subjected to the sensor error, we obtain the heat injection rate per unit length of the BHE using the following equation:

$$q = \rho c \dot{V} (T_{in} - T_{out})/H \quad (1)$$

Here, ρ represents the density of the circulating fluid, c the specific heat capacity of fluid, $\dot{V}$ the volumetric flow rate of fluid, H the length of the BHE, and T_{in} and T_{out} the inlet and outlet fluid temperatures, respectively.

Table 1. Parameters of borehole heat exchanger (BHE) used for numerical thermal response test (TRT).

Component	Parameter [units]	Value
Water	Thermal conductivity [W/(m·K)]	0.6
	Volumetric thermal capacity [MJ/(m^3·K)]	4.2
U-tube (High density polyethylene)	Outer diameter [mm]	34
	Inner diameter [mm]	27
	Shank spacing [mm]	50
	Thermal conductivity [W/(m·K)]	0.36
	Volumetric thermal capacity [MJ/(m^3·K)]	1.8
Borehole	Borehole depth [m]	50
	Borehole diameter [mm]	165
Grout	Thermal conductivity [W/(m·K)]	1.4
	Volumetric thermal capacity [MJ/(m^3·K)]	2.0
Ground	Thermal conductivity [W/(m·K)]	1.8
	Volumetric thermal capacity [MJ/(m^3·K)]	2.5

3. Parameter Estimation

3.1. Physical model

To perform the inverse parameter estimation, it is necessary to apply a physical model that can reproduce the problem of interest. We used the infinite line source (ILS) model [2,3] in our study. This analytical model was derived from the 1D heat equation with the boundary condition of constant heat flux from the line source. Via application of temporal superposition to the heat flux, the disturbed heat rate can be considered more accurately. The ILS model with respect to the average fluid temperature F (i.e., the arithmetic average of inlet and outlet temperatures) can be expressed as:

$$F = \sum_{n=1}^{N} \frac{q_n - q_{n-1}}{4\pi\lambda_{eff}} \mathrm{Ei}\left(\frac{C_s r_b^2}{4\lambda_{eff}(t_N - t_{n-1})}\right) + R_b q_N + T_0 \quad (2)$$

Here, q_n represents the heat pulse at time step n, λ_{eff} the effective thermal conductivity, C_s the volumetric thermal capacity of the ground, t_N the final time of the test, R_b the borehole thermal resistance, q_N the final heat pulse, and T_0 the initial ground temperature.

Although the ILS model assumes a homogeneous ground, the components within the BHE have different thermal properties. Therefore, an early-time temperature response is not reliable, and thus, we only used temperature data from the elapsed time of 15 h for both estimation methods.

3.2. Parameters

We define parameter vector **P** that contains λ_{eff} and R_b as follows.

$$\mathbf{P} = (\lambda_{eff}, R_b) \tag{3}$$

In addition, we define parameter r_σ that quantifies that the error ratio between the measured temperature Y and modeled temperature F normalized by reference temperature difference between the measured temperature Y and initial ground temperature T_0.

$$r_\sigma = \left|\frac{Y - F}{Y - T_0}\right| \tag{4}$$

It should be noted that r_σ denotes the error ratio between the measured temperature subjected to the measurement error and the modeled temperature that cannot perfectly reproduce the physical phenomenon of interest, and further, r_σ is not the deviation from the true temperature. Because we do not have any plausible basis in setting r_σ, we consider it as a hyperparameter to be estimated in addition to **P**.

3.3. Bayesian inference method

Based on the Bayes' theorem, we can express the conditional probability of parameter vector **P** as follows:

$$p(\mathbf{P}, r_\sigma|Y) = \frac{p(Y|\mathbf{P}, r_\sigma)p(\mathbf{P}, r_\sigma)}{p(Y)} \tag{5}$$

Here, $p(\mathbf{P}, r_\sigma|Y)$ represents the posterior distribution given the measured data Y, $p(Y|\mathbf{P}, r_\sigma)$ the likelihood of **P** and r_σ given Y, $p(\mathbf{P}, r_\sigma)$ the prior of the uncertain parameters, and $p(Y)$ the evidence.

The value of evidence $p(Y)$ is very difficult to determine; however, we know that it is a constant. Therefore, Eq. (5) can be rewritten as the following proportional expression without the denominator of right-hand side.

$$p(\mathbf{P}, r_\sigma|Y) \propto p(Y|\mathbf{P}, r_\sigma)p(\mathbf{P}, r_\sigma) \tag{6}$$

3.3.1. Likelihood

We make estimations by comparing the measured and modeled temperatures while noting that both temperatures have uncertainties. The measurement error e_y originates from the intrinsic error of the sensors and the model error e_f originates due to model inadequacy and numerical error. If we assume the unknown true temperature as $\bar{T}_{tr}$, the measured and modeled temperatures that are subjected to error can be expressed as Eqs. (7) and (8), respectively.

$$Y = \bar{T}_{tr}^n + e_y^n \tag{7}$$

$$F^n = \bar{T}_{tr}^n + e_f^n \tag{8}$$

Here, the superscript n describes the time step.

The measurement and model errors were assumed to follow a normal distribution with a mean of zero and variances of $\sigma_{y,n}^2$ and $\sigma_{f,n}^2$, respectively. Under these assumptions, the likelihood functions with respect to the measured temperature and true temperature are expressed as Eq. (9) and Eq. (10), respectively.

$$p(Y|\bar{T}_{tr}) = \prod_{n=1}^{N} \frac{1}{\sqrt{2\pi\sigma_{y,n}^2}} \exp\left[-\frac{(Y^n - \bar{T}_{tr}^n)^2}{2\sigma_{y,n}^2}\right] \tag{9}$$

$$p(\bar{T}_{tr}|\mathbf{P}) = \prod_{n=1}^{N} \frac{1}{\sqrt{2\pi\sigma_{f,n}^2}} \exp\left[-\frac{\left(\bar{T}_{tr}^n - F^n(\mathbf{P})\right)^2}{2\sigma_{f,n}^2}\right] \tag{10}$$

Here, N denotes the total number of time steps.

With the use of the two predefined likelihood functions, the likelihood $p(Y|\mathbf{P})$ can be written as follows:

$$p(Y|\mathbf{P}) = \int_{\text{all } \bar{T}_{tr}} p(Y|\bar{T}_{tr}) p(\bar{T}_{tr}|\mathbf{P})\, \mathrm{d}\bar{T}_{tr} \tag{11}$$

Equation (11) describes the marginalization of the likelihood with respect to the unknown $\bar{T}_{tr}$. Upon substituting Eqs. (9) and (10) in Eq. (11), we can obtain the following marginalized likelihood function.

$$p(Y|\mathbf{P}) = \prod_{n=1}^{N} \frac{1}{\sqrt{2\pi\left(\sigma_{y,n}^2 + \sigma_{f,n}^2\right)}} \cdot \exp\left[-\frac{1}{2}\sum_{n=1}^{N} \frac{\left(Y^n - F^n(\mathbf{P})\right)^2}{\sigma_{y,n}^2 + \sigma_{f,n}^2}\right] \tag{12}$$

If we know the measurement and model errors, measured temperature, and modeled temperature, the likelihood $p(Y|\mathbf{P})$ can be calculated. Among the variables in Eq. (12), the measurement and model errors are difficult to quantify. We set the sum of the two variances as a hyperparameter to be estimated. By introducing the new variable, the error ratio r_σ, the magnitude of the sum of the two variances can be defined as shown in Eq. (13).

$$\sigma_{y,n}^2 + \sigma_{f,n}^2 \approx \left(r_\sigma (Y^n - T_0)\right)^2 \tag{13}$$

As described previously (Eq. (4)), r_σ denotes the error ratio of the modeled temperature with respect to the measured temperature. Upon substituting Eq. (13) into Eq. (12), the likelihood function can be rewritten as follows:

$$p(Y|\mathbf{P}, r_\sigma) \propto \frac{1}{r_\sigma^N} \exp\left[-\frac{1}{2}\sum_{n=1}^{N} \frac{\left(Y^n - F^n(\mathbf{P})\right)^2}{\left(r_\sigma (Y^n - T_0)\right)^2}\right] \tag{14}$$

3.3.2. Prior

In deciding the prior distribution of the estimation parameters λ_{eff}, R_b, and r_σ, we can speculate their range based on certain prior information. For example, the range of λ_{eff} can be decided from the drill log of the borehole or past soil sampling data near the site. In the case of R_b, we can resort to a calculation model. Of course, TRT results based on a deterministic approach can also be used to determine their range. Regarding the error ratio r_σ, we know that it is a positive definite value, and the upper bound can be set using an arbitrarily large value such as 0.2. We thus set the ranges of parameters as follows:

$$\begin{gathered} 1.0 \le \lambda_{eff} \le 3.0 \\ 0.14 \le R_b \le 0.18 \\ 0 \le r_\sigma \le 0.2 \end{gathered} \tag{15}$$

However, specifying the probability distributions of estimation parameters requires considerable information, which may not be available. Therefore, we set the probability as constant in the parameter space $\Re$.

$$p(\mathbf{P}, r_\sigma) = \text{constant}, (\mathbf{P}, r_\sigma) \in \Re \tag{16}$$

3.3.3. Posterior using Markov chain Monte Carlo method

Because we set the priors as constant, the posterior only depends on the likelihood. In addition, our restriction on the parameter space can be considered in the calculation of the posterior with the use of an indicator function I. The final form of the posterior probability including the indicator function can be expressed as follows:

$$p(\mathbf{P}, r_\sigma|Y, I) \propto p(Y|\mathbf{P}, r_\sigma, I)p(\mathbf{P}, r_\sigma|I) \propto I\big((\mathbf{P}, r_\sigma) \in \Re\big)\frac{1}{r_\sigma^N}\exp\left[-\frac{1}{2}\sum_{n=1}^{N}\frac{\big(Y^n - F^n(\mathbf{P})\big)^2}{\big(r_\sigma(Y^n - T_0)\big)^2}\right] \tag{17}$$

The posterior $p(\mathbf{P}|Y)$ can be evaluated by means of the Markov chain Monte Carlo (MCMC) method; we used the Metropolis–Hastings algorithm [4,5] in our study. When a sampled parameter was out of the parameter space, the indicator function I becomes zero, and thus, the sampled parameter of the current step $\mathbf{P}^k$ was abandoned and the parameter in the previous step was used in the next iteration, $\mathbf{P}^k \leftarrow \mathbf{P}^{k-1}$. From an arbitrary initial parameter vector, $\mathbf{P}^0$, and r_σ, sampling was repeated 6×10^5 times. Because the early iteration steps strongly depend on the initial values, the first 1×10^5 samples were neglected and the subsequent 5×10^5 samples were used for the posterior distribution.

3.3.4. Two-step sampling method

In general, a simultaneous estimation of λ_{eff} and R_b is possible because these parameters exhibit independent transient behavior of the sensitivity coefficient, as examined in Ref. [6]. However, for the ill-posed characteristic of the inverse problem, infinite combinations of λ_{eff} and R_b can yield the same result when limited experimental data are used for estimation. If an estimation is made with a gradient-based search algorithm with a suitable initial value that is close to the true value, the estimation will converge to a local minimum near the true point. However, when the MCMC is used, the estimation becomes difficult because the MCMC is a sort of random search method that is similar to a heuristic-based search algorithm. Consequently, the sampling results would be distributed all over the parameter space and show a multimodal distribution.

To overcome this difficulty, we applied a two-step sampling method. Firstly, the sampling of λ_{eff} and r_σ was obtained with the use of a constant R_b. This R_b value can be determined from a conventional deterministic method with measured TRT data or analytical models for R_b. After the sampling of λ_{eff} and r_σ was completed, as the second step, R_b was sampled with the pre-sampled λ_{eff} value. The λ_{eff} value was retrieved in the sampled sequence; when the iteration step of R_b was 100, the 100th sampled value in the λ_{eff} vector was retrieved. In the process of R_b sampling, r_σ was also sampled again with the retrieved λ_{eff} and sampled R_b. This method facilitates the probabilistic estimation of the three parameters.

3.4. Deterministic estimation: quasi-Newton method

In addition to the Bayesian probabilistic estimation method, we also obtained conventional deterministic estimations as part of our study. The quasi-Newton method was used for inverse parameter estimation. The Broyden–Fletcher–Goldfarb–Shanno (BFGS) algorithm was used to approximate the Hessian. The details of this estimation method can be found in Ref. [7].

Three conditions are used as general stopping criteria for the iteration procedure: (1) the objective function, $f_{obj}(\mathbf{P}^k)$, reaches a predefined tolerance of 10^{-5}, (2) the iteration reaches the maximum number of iterations, or (3) the difference of two consecutive estimates $|\mathbf{P}^k - \mathbf{P}^{k-1}|$ falls below a predefined value.

4. Results

The red dash-dot line in Fig. 1 shows the measured temperature response. We discuss the modeled temperatures in a later section of the paper. The measured temperature is affected by the error of the temperature sensors only and not affected by the random error of the flow meter. Here, we remark that it is easy to mistake the error of the flow sensor for the measurement error. However, the flow sensor error should be considered as the modeled error because the measured flow rate is used to obtain the heat rate q, and it is used for predicting the temperature response. With the use of the generated response data without error and measured data (affected by error), we utilized the conventional deterministic interpretation that is based on the approximated ILS model to estimate λ_{eff} and R_b (i.e., the estimation method using a gradient of temperature versus log time plot). The estimated λ_{eff} and R_b values with the use of the "clean" and measured data were 1.79 W/m·K and 0.163 m·K/W, and 1.78 W/m·K and 0.165 m·K/W, respectively.

To generate the posterior probability distribution of the parameters, we performed two-step MCMC sampling 6×10^5 times. The first step of λ_{eff} sampling was performed with the deterministically estimated R_b value of 0.165 m·K/W. After the sampling of λ_{eff} was completed, the sampling of R_b and updating of r_σ were performed. Because the sampled results of the initial iterations were strongly affected by the initial values of the parameters, the first 1×10^5 samples were omitted; the rest 5×10^5 sampled data values of λ_{eff}, R_b, and r_σ are shown in Fig. 2. The red dash-dot line represents the true value of each parameter. For both λ_{eff} and R_b, the generated samples fluctuate around the true value, and the center of the sampled range is close to the true value (Figs. 2(a) and (b)). As regards r_σ, the generated samples exhibit prominent peaks only in the upper region and are always larger than 2.4%.

Using the 5×10^5 sampled data sets shown in Fig. 2, we constructed the posterior probability density functions (PDFs) and box plots. The PDFs and box plots of λ_{eff} and R_b are shown in Fig. 3 and those of r_σ are shown in Fig. 4. The PDFs of λ_{eff} and R_b exhibit a normal distribution that is almost symmetric, and the true value is included in the range of the first and third quartiles (within the box of the box plot). In contrast to the PDFs of λ_{eff} and R_b, we observe a slight skewness (the relatively longer tail in the upper region) in the PDF of r_σ. From this PDF, we speculate that the temperature error between the measurement and model is mostly in the range of 5–7%, but sometimes it can increase by 8%. This relatively large error can occur at a time when the random

errors of inlet and outlet temperature sensors work in opposition (e.g., positive and negative errors are added to the inlet and outlet sensors, respectively) and a large random error of the flow meter occurs.

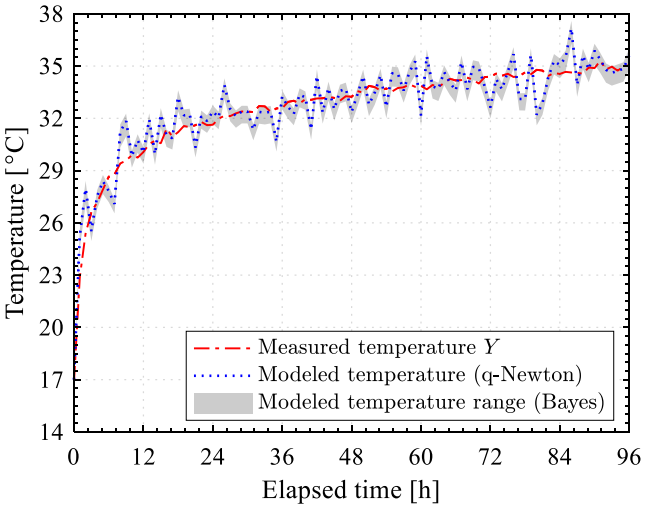


Fig. 1. Measured and modeled temperature responses with the use of parameters from different estimation methods.

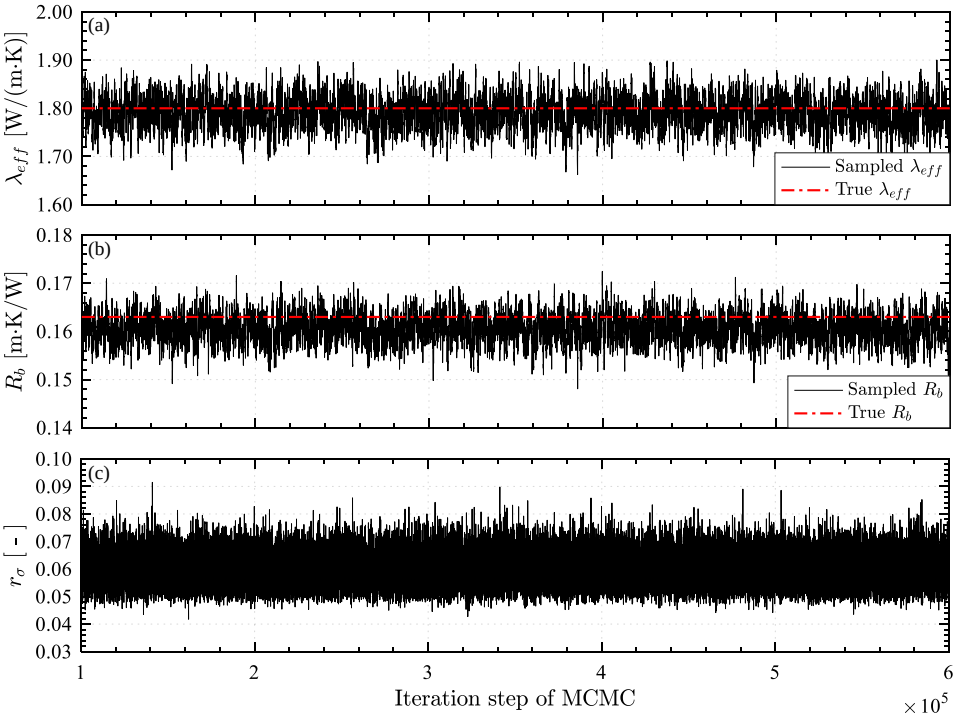


Fig. 2. Sampled results of parameters; (a) effective thermal conductivity (true value = 1.8 W/(m·K)), (b) borehole thermal resistance (true value = 0.163 m·K/W), and (c) error ratio.

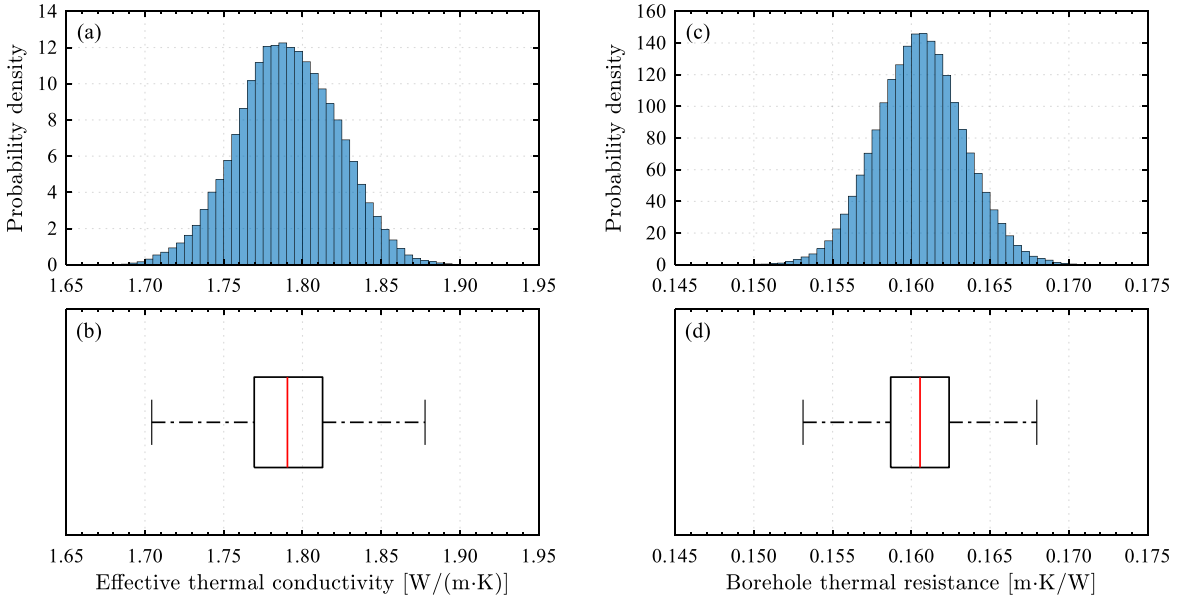


Fig. 3. Normalized probability density functions and box plots. (a) Probability density function (PDF) of λ_{eff}, (b) box plot of λ_{eff}, (c) PDF of R_b, and (d) box plot of R_b. The lower and upper ends of the box represent the first and third quartiles, respectively, and the red band inside the box denotes the median. The left and right ends of the whiskers represent q_1 - 1.5(q_3 - q_1) and q_3 + 1.5(q_3 - q_1), respectively. Outliers are not shown in the box plot.

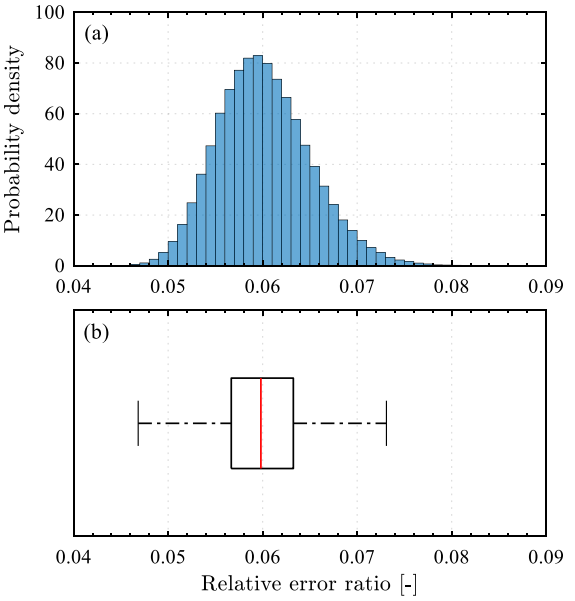


Fig. 4. Normalized probability density function and box plot of r_σ.

Table 2 summarizes the parameters estimated from both the Bayesian and deterministic approaches. The midpoint of the most frequent interval of each parameter's PDF was considered to be the estimated value from the Bayesian inference. Although the estimated λ_{eff} and R_b values are slightly smaller than the corresponding true values, the estimated values are very close to the true values and within the 95% confidence intervals. The estimation from the deterministic method also provides estimates that are very close to the true value. The estimated range of the error ratio provides a good insight into the relative deviation between the measured and modeled temperatures.

With the use of the estimated parameters from the two estimation approaches and the measured heat rate, the temperature response was reproduced with the ILS model, as shown in Fig. 1. As described previously, the error of the flow meter works as the model error, and the modeled temperature exhibits very unstable behavior. Although the modeled temperature response fluctuates significantly, the PDFs exhibited a strong unimodality with a short tail because the fluctuating heat rate was considered using the temporal superposition of heat rate. However, if the temperature response is disturbed further by disturbance factors from the ambient environment in addition to the sensor errors and the TRT data are interpreted with the use of conventional regression method assuming an averaged constant heat rate, then the estimation results can become very unstable and the error becomes large.

Table 2. Estimated parameters obtained with different methods.

Parameter [unit]	Bayesian (95% confidence interval)	Quasi-Newton
Effective thermal conductivity [W/(m·K)]	1.79 (1.73–1.85)	1.79
Borehole thermal resistance [m·K/W]	0.161 (0.156–0.167)	0.164
Error ratio [%]	6.0 (5.1–7.1)	N/A

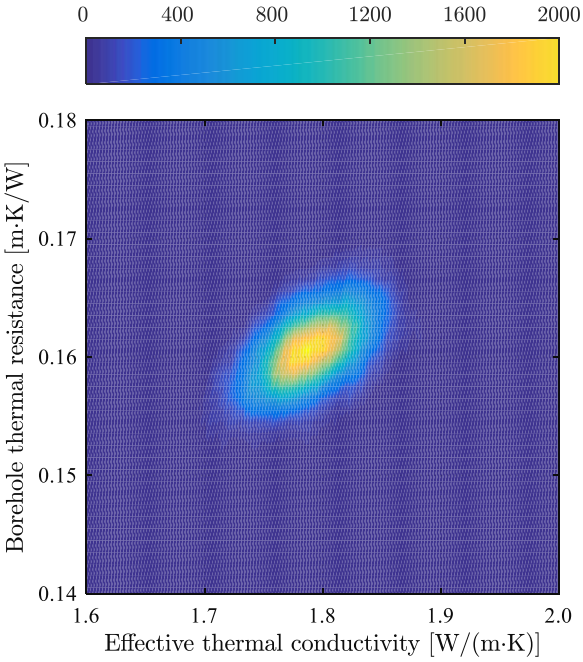


Fig. 5. Joint probability density function

Although we fortunately obtained parameters very close to the true values in our study, we note the possibility of obtaining biased results due to the influence of various uncertain factors. The bias of estimation is difficult to identify from the developed method because we can never determine a true value. However, in contrast to a deterministic estimation approach, a probabilistic approach can provide a confidence interval and the probability distribution of the estimated parameter. Via exploiting these advantages of the probabilistic estimation method, we can account for the risk arising from any bias in the design of the GSHP.

An additional advantage of the Bayesian approach is that it can yield a joint probability density function when two or more parameters are estimated simultaneously. From the joint PDF shown in Fig. 5, we can determine the correlation of the two parameters and the area where the most reliable pairs of parameters exist. The parameter combinations in the yellow area represent the most reliable pairs of λ_{eff} and R_b, and these exhibit a proportional relation.

5. Conclusions

In this study, we reproduced a TRT using an FEM, and we estimated the effective thermal conductivity, borehole thermal resistance, and error ratio between the measured and modeled temperatures using the probabilistic Bayesian and deterministic quasi-Newton methods. Both methods could estimate parameters that were very close to the true values. However, the Bayesian approach is superior to the deterministic method because it can potentially consider possible errors that affect inverse estimation results and can provide a possible range and probability distribution for the estimated parameters. Further research regarding the potential of the Bayesian approach for different problem configurations and application to in situ experiments will be conducted in the future.

Acknowledgements

This work was supported by the Japan Society for the Promotion of Science (JSPS) KAKENHI, grant numbers 26709041 and P16074.

References

[1] W. Choi, R. Ooka, Effect of disturbance on thermal response test, part 2: Numerical study of applicability and limitation of infinite line source model for interpretation under disturbance from outdoor environment, Renew. Energy. 85 (2016) 1090–1105.

[2] H.S. Carslaw, J.C. Jaeger, Conduction of Heat in Solids, 2nd ed., Oxford University Press, UK, 1959.

[3] L.R. Ingersoll, O.J. Zobel, A.C. Ingersoll, Heat conduction with engineering, geological, and other applications, University of Wisconsin Press, Madison, 1954.

[4] N. Metropolis, A.W. Rosenbluth, M.N. Rosenbluth, A.H. Teller, E. Teller, Equation of State Calculations by Fast Computing Machines, J. Chem. Phys. 21 (1953) 1087.

[5] W.K. Hastings, Monte Carlo sampling methods using Markov chains and their applications, Biometrika. 57 (1970) 97–109.

[6] W. Choi, R. Ooka, Effect of natural convection on thermal response test conducted in saturated porous formation: Comparison of gravel-backfilled and cement-grouted borehole heat exchangers, Renew. Energy. 96 (2016) 891–903.

[7] W. Choi, R. Ooka, Interpretation of disturbed data in thermal response tests using the infinite line source model and numerical parameter estimation method, Appl. Energy. 148 (2015) 476–488.